

# PLoRA: Efficient LoRA Hyperparameter Tuning for Large Models

Minghao Yan<sup>\*†</sup>  
University of Wisconsin-Madison

Zhuang Wang<sup>†</sup>  
Amazon Web Services

Zhen Jia  
Amazon Web Services

Shivaram Venkataraman  
University of Wisconsin-Madison

Yida Wang  
Amazon Web Services

## Abstract

Low-rank Adaptation (LoRA) has gained popularity as a fine-tuning approach for Large Language Models (LLMs) due to its low resource requirements and good performance. While a plethora of work has investigated improving LoRA serving efficiency by serving multiple LoRAs concurrently, existing methods assume that a wide range of LoRA adapters are available for serving. In our work, we conduct extensive empirical studies to identify that current training paradigms do not utilize hardware resources efficiently and require high overhead to obtain a performant LoRA. Leveraging these insights, we propose PLoRA, which automatically orchestrates concurrent LoRA fine-tuning jobs under given hardware and model constraints and develops performant kernels to improve training efficiency. Our experimental studies show that PLoRA reduces the makespan of LoRA fine-tuning over a given hyperparameter search space by up to 7.52 $\times$  and improves training throughput by up to 12.8 $\times$  across a range of state-of-the-art LLMs.

## 1 Introduction

Large Language Models (LLMs) have become the backbone of numerous modern AI applications, spanning natural language understanding, code generation, multimodal reasoning, and specialized domains such as healthcare and finance [20, 23, 50]. The paradigm of pre-training followed by fine-tuning has enabled these models to achieve state-of-the-art performance when adapted to specific tasks [40].

However, fine-tuning large models for multiple tasks or user-specific applications poses a significant challenge due to the high computational cost of training and serving numerous fine-tuned variants. To address this, parameter-efficient fine-tuning (PEFT) techniques such as Low-Rank Adaptation (LoRA) [25] have emerged as scalable alternatives to full fine-tuning. LoRA significantly reduces the number of trainable parameters by introducing low-rank decomposition matrices into Transformer layers, allowing for specialization while keeping the pre-trained model weights frozen. This versatile deployment approach has become popular, and several systems have been recently developed to serve multiple LoRA adapters concurrently [9, 43]. LoRA fine-tuning is also widely

adopted in mainstream ML frameworks [37, 46]. Companies like Apple [22] have employed LoRA in their on-device language models to facilitate task-specific adaptation (e.g., email summarization or image captioning) while maintaining a lightweight memory footprint. Although initially developed for adapting language models, LoRA is also widely used in other domains, such as diffusion models for image generation [33, 42] and large vision-language models [34].

Existing LoRA-related inference systems, such as vLLM [31], SLoRA [43], and LoRAX [51], operate under the assumption that LoRA adapters are already well-trained and a LoRA checkpoint with decent model quality is available for a given downstream task. In this paper, we focus on the question of *how to train such LoRA adapters efficiently*.

Similar to other deep learning methods, we find that the effectiveness of LoRA fine-tuning hinges on selecting appropriate hyperparameters (§2.2). In the context of LoRA, hyperparameter tuning extends beyond standard parameters, such as learning rate and batch size. LoRA-specific parameters that need to be tuned include: 1. LoRA rank, which controls the dimensionality of the adapter matrices. A higher rank increases the expressive power but comes at a higher memory and computation cost [25]. 2. A scaling factor  $\alpha$ , which determines the impact of the LoRA adapters on the pre-trained weights. We conduct a large-scale empirical study and demonstrate that there is no single rule of thumb for tuning LoRA hyperparameters. Through more than 1,000 experiments, we demonstrate that different tasks (e.g., mrpc [47], gsm8k [10]) require different hyperparameter configurations to achieve optimal performance on various base models, highlighting the need for LoRA hyperparameter tuning.

However, traditional hyperparameter tuning techniques [6, 7, 28] only focus on reducing the number of tuning runs and do not account for the unique characteristics of LoRA adapters, leading to significant inefficiencies. LoRA adapters are **heterogeneous** and have **varying resource requirements** (§2.3), enabling intra-run optimization opportunities. We find that many LoRA configurations evaluated during hyperparameter tuning have small batch sizes and underutilize GPU hardware resources, with SM occupancy around 16.7% and memory utilization less than 55%. Based on these observations, we propose *packing multiple LoRA configurations* during hyperparameter tuning, thereby sharing hardware

<sup>\*</sup>Work done during an internship at Amazon Web Services.

<sup>†</sup>Equal contribution.

resources across configurations and improving hardware utilization.

We develop PLoRA, an automated concurrent LoRA training system. Given a base model and a predefined hyperparameter search space, PLoRA orchestrates efficient LoRA fine-tuning jobs and executes them with packed LoRA adapters. PLoRA operates in two stages: an offline planning stage followed by an online execution stage. We first design an offline packing planner that analyzes the hyperparameter search space and creates jobs with packed LoRA configurations that maximize throughput. The planner also determines the appropriate degree of parallelism for each job. We formulate the planner as an optimization problem and design an efficient approximate algorithm with provable performance bounds (§6).

In the second stage, the jobs created by the planner are deployed by an online LoRA Execution Engine. The execution engine monitors available hardware resources and launches multiple tuning jobs concurrently if sufficient resources are available. We also design new GPU kernels for packed LoRA adapters that are used once a job is launched, and show that our kernels can achieve near-linear speedups for up to 32 adapters across various base models (§5).

In summary, we make the following contributions:

- We conduct a large-scale empirical study with more than 1,000 experiments to demonstrate the necessity of optimizing LoRA hyperparameter tuning.
- We develop an algorithm to automatically allocate multiple LoRA fine-tuning tasks to jobs while accounting for hardware, model, and LoRA configuration constraints.
- We design efficient concurrent LoRA fine-tuning kernels that achieve near-linear speedup when training more than 32 adapters simultaneously.
- We implement PLoRA, a parallel LoRA fine-tuning framework that significantly accelerates training compared to baseline methods.
- We evaluate PLoRA using four different base models and show that while tuning more than 100 configurations, PLoRA reduces the total hyperparameter tuning makespan by up to 7.52×

## 2 Hyperparameter Tuning in LoRA

### 2.1 Low-Rank Adaptation (LoRA)

Fine-tuning a pre-trained model is usually needed to obtain domain knowledge for different tasks and is repeated when the dataset or task requirements change [14, 24]. Low-Rank Adaptation (LoRA) [25] is a widely adopted efficient fine-tuning technique for Large Language Models (LLMs). LoRA dramatically reduces the number of parameters that need to be trained by freezing the original model weights, i.e., *base model*, and only introducing trainable low-rank decomposition matrices, i.e., *LoRA adapter*, which is much smaller than

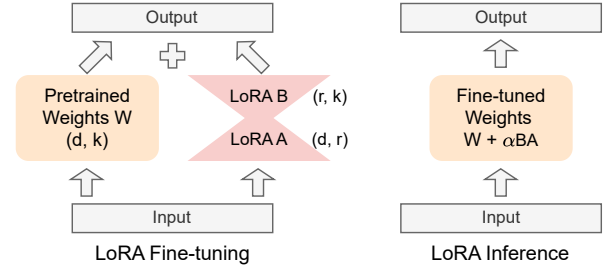


**Figure 1.** This figure demonstrates how LoRA is applied to weight matrices in fine-tuning and inference.

**Table 1.** Hyperparameters for LoRA fine-tuning.

Hyperparameters	Search range	Meaning
Learning rate (LR)	2e-5 ~ 4e-4	Step size for weight updates
Batch size (BS)	1 ~ 32	# samples in a batch
LoRA rank (r)	8 ~ 128	LoRA decomposition rank
LoRA alpha ( $\alpha$ )	$r/4 \sim 4r$	LoRA scaling factor

the base model. Formally, for a weight matrix  $W \in \mathbb{R}^{d \times k}$ , LoRA adds the weight updates  $\Delta W$  as two small matrices  $A \in \mathbb{R}^{d \times r}$  and  $B \in \mathbb{R}^{r \times k}$ , where  $r$  is the LoRA rank and it is much smaller than  $d$  and  $k$ . The additional FLOPs incurred by LoRA is linear to its rank. LoRA only updates  $A$  and  $B$ , thus significantly reducing computation and storage costs for model fine-tuning. For instance, a LoRA adapter with rank 64 on QWen-2.5-7B only updates 3.4% of the model parameters. During inference, LoRA merges the multiplied matrix  $\Delta W = B \times A$  into the original weight matrix  $W$  with a scaling factor LoRA alpha  $\alpha$  and the weight matrix becomes  $W = W + \alpha \Delta W$ , as shown in Figure 1.

### 2.2 Hyperparameter space

Hyperparameter tuning is a fundamental process in developing deep learning models, involving selecting optimal values for parameters not learned during training [6]. These hyperparameters include, but are not limited to, the *learning rate*, which determines the step size for updating model weights, and the *batch size*, which defines the number of samples processed before a weight update. LoRA fine-tuning also requires hyperparameter tuning and introduces additional hyperparameters, such as *LoRA rank* and *LoRA alpha*, which are specifically related to LoRA adapters. The set of hyperparameters studied in this paper for LoRA fine-tuning is listed in Table 1. Introducing these LoRA-specific hyperparameters expands the search space of hyperparameter tuning, making the process more complex and challenging.

### 2.3 Study of LoRA Hyperparameter Tuning

We perform an extensive empirical study of the impact of hyperparameters on model quality with LoRA fine-tuning. The

**Table 2.** Each LoRA hyperparameter can affect the downstream accuracy. The base model is QWen-2.5-7B. We only tune one hyperparameter and keep the others fixed. The results are the maximum accuracy differences by tuning the chosen hyperparameter.

Task	LR	BS	LoRA rank	$\alpha$
mrpc	8.5%	10.0%	6.4%	4.9%
cola	14.2%	8.5%	13.1%	5.9%
wnli	6.8%	11.3%	5.4%	5.5%
gsm8k	5.0%	3.2%	4.5%	2.5%

**Table 3.** Model quality of QWen-2.5-7B with the base model only, the worst, and the best LoRA hyperparameter configuration across various tasks. Improve represents the accuracy difference between the best configuration and the base model.

	Base model	Worst	Best	Improve
mrpc	64.1%	57.1%	70.0%	5.9%
cola	62.7%	61.5%	80.2%	18.5%
wnli	78.8%	74.7%	84.5%	5.7%
gsm8k	70.8%	71.2%	79.8%	8.0%

detailed experimental setup is described in §7. We use QWen-2.5 [50] as the base model and report the zero-shot accuracy on the following benchmarks in our experiments: **GSM8K** [10] for mathematical reasoning; **mrpc** [47] for language understanding; **cola** [47] for commonsense reasoning; and **wnli** [47] for logic reasoning.

**Observation #1: Every hyperparameter affects model quality.** To investigate the impact of each hyperparameter on model quality, we only change one of the four hyperparameters listed in Table 1 with the specified search ranges while fixing the others with the optimal hyperparameter configurations found in 4. We list the model quality in Table 2.

We find that varying the learning rate can cause a difference of up to 14.2% in model accuracy, while varying batch size, LoRA rank, and LoRA alpha can cause differences of up to 11.3%, 13.1%, and 5.9%, respectively.

**Observation #2: All hyperparameters collectively influence model quality significantly.** We study the hyperparameters’ collective impact on model quality. For simplicity, we define a *LoRA configuration* as a set of values for the four hyperparameters. We run 120 LoRA configurations from the search space for each downstream task by building a grid based on the ranges specified in 1. In Table 3, we compare the accuracy of a pre-trained QWen-2.5-7B base model with LoRA fine-tuned models. Although we expect LoRA fine-tuning to enhance model quality on specific tasks, surprisingly we find that LoRA configurations can worsen model accuracy without careful tuning. For example, the accuracy of the pre-trained base model is 78.8% for wnli, but the worst LoRA configuration degrades it to 74.7%.

**Table 4.** This table shows the optimal hyperparameter configuration we found during the hyperparameter sweep. The table shows that the optimal configuration varies by task and base model, warranting careful tuning of LoRA hyperparameters.

Task	3B				7B			
	Rank	LR	BS	$\alpha$	Rank	LR	BS	$\alpha$
mrpc	16	4e-5	1	1	32	6e-5	1	1
cola	64	4e-4	1	0.25	32	8e-5	1	0.5
wnli	32	2e-4	2	1	32	2e-4	4	0.5
gsm8k	32	1e-4	2	1	16	3e-4	1	1

By searching among 120 LoRA configurations, LoRA fine-tuning improves the accuracy for cola, wnli, and gsm8k by 18.5%, 5.7%, and 9.0%, respectively.

**Observation #3: Different LoRA fine-tuning workloads require different configurations.** We also study how the best LoRA configurations vary across different LoRA fine-tuning workloads, which are evaluated using both QWen-2.5-3B and QWen-2.5-7B as base models. The best LoRA configurations for different workloads are listed in Table 4.

We show that the best hyperparameter configurations for LoRA fine-tuning differ by task. For example, for QWen-2.5-3B, the best configuration for mrpc is [16, 4e-5, 1, 1], but is [32, 1e-4, 2, 1] for gsm8k. When we apply the best configuration for mrpc to gsm8k, the model accuracy for gsm8k degrades by 7.4%.

We also find that the best LoRA configurations for a given task differ by the base models. When we apply the best configuration on QWen-2.5-7B for cola to QWen-2.5-3B, the model accuracy degrades by 3.6%.

**Observation #4: LoRA Fine-tuning prefers small batch sizes.** We observe that LoRA fine-tuning consistently yields better model accuracy when using smaller batch sizes than larger ones. Table 4 shows that LoRA prefers a small batch size ( $\leq 4$ ). This observation aligns with the practical batch size settings in LoRA fine-tuning [16, 25, 51]. A smaller batch size inherently reduces the variance of the gradient estimate when only a fraction of the parameters are updated, which can be beneficial for convergence and generalization [25]. We observe similar trends in other hyperparameter settings when we only vary batch sizes.

### 3 Efficient LoRA Hyperparameter Tuning

Next, we investigate the system efficiency of LoRA fine-tuning. We first discuss systems challenges in searching for the best LoRA configuration in a large search space. We then propose a new LoRA fine-tuning paradigm that significantly optimizes throughput for LoRA hyperparameter tuning, and discuss some new systems challenges that arise.

### 3.1 Hardware Underutilization

**SM underutilization.** We profile the SM occupancy for single LoRA fine-tuning with Nsight Compute on one A100 GPU with QWen-2.5-7B as the base model on Unsloth [11]. While we vary batch size from 1 to 16 and rank from 8 to 128, the SM occupancy remains constant at 16.7% for both base model and LoRA kernels. We also observe a similar phenomenon when performing LoRA fine-tuning on QWen-2.5-3B using one A10 GPU. This constant low occupancy arises because kernels use a large amount of shared memory and registers, which limits each SM to host only one thread block. Heavy shared memory usage can benefit large, compute-dense base model kernels by reusing data in shared memory for computation. In contrast, LoRA’s much smaller matrices lack the arithmetic intensity and shared memory data reuse needed to fully utilize the tensor cores, suggesting that most SM resources sit idle during adapter updates.

**Memory underutilization.** When a single LoRA configuration is fine-tuned for a given set of hardware resources, GPU memory is often also underutilized. This underutilization arises from two factors: 1) The base model remains frozen, so only the relatively small LoRA adapter is updated, and 2) LoRA fine-tuning typically uses small batch sizes, further reducing memory demand.

As discussed in §2.3, to find a well-trained LoRA adapter, it is necessary to search for the best LoRA configuration from a large search space, e.g., 120 configurations used in §7. However, the low hardware utilization makes it difficult to fully leverage the available resources for evaluating all LoRA configuration candidates.

**Existing hyperparameter tuning approaches fall short.** Several techniques, such as grid search [6], random search [7], and Bayesian optimization [28], have been proposed for efficient hyperparameter tuning. However, these techniques only focus on reducing the number of tuning runs and are agnostic to the time taken or resources required for each configuration. Thus, when applying these approaches to LoRA fine-tuning, the hardware resource is still underutilized during each LoRA configuration run.

### 3.2 Our Proposal: LoRA Fine-tuning with Packed LoRA Configurations

Given a set of hardware resources for model hyperparameter tuning, existing approaches [6, 7, 28] can concurrently evaluate multiple configurations by dividing the resources into disjoint units, each running on a dedicated unit. However, they cannot run multiple configurations on a resource unit simultaneously. Another configuration must wait for the hardware resource until the previous one finishes the fine-tuning workload.

In this paper, we propose packing multiple LoRA configurations for simultaneous fine-tuning, thereby sharing the same hardware resources to improve hardware utilization.

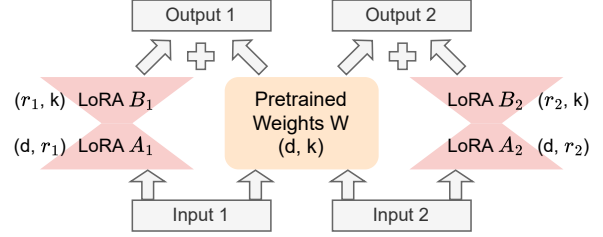


**Figure 2.** This figure demonstrates how PLoRA works with two LoRA adapters packed in a fine-tuning job. Each LoRA adapter receives a distinct input, which is processed independently by the shared base model and the corresponding LoRA adapter. The outputs from the base model and each LoRA adapter are then merged independently for each input.

**Packing LoRA adapters is feasible.** Each LoRA configuration corresponds to a distinct LoRA adapter, while the base model remains identical across all configurations, as its weights are frozen during LoRA fine-tuning. This insight motivates the idea of packing multiple LoRA configurations into a single fine-tuning job, thereby avoiding out-of-memory (OOM) issues. Packing LoRA adapters is feasible because: 1) Each LoRA adapter is significantly smaller than the base model, and 2) Memory usage during LoRA fine-tuning is largely dominated by the (frozen) base model weights. For instance, using QWen-2.5-7B as the base model, the LoRA adapter of rank 64 is 243MB, which is only 3.4% of the base model size. When we pack two LoRA adapters for QWen-2.5-7B on a single A100 GPU, the memory usage increases from 18.2GB (with one adapter) to 20.4GB (including activation and optimizer memory); thus, we can accommodate up to 10 concurrent LoRA adapters without OOM errors. When performing distributed fine-tuning (e.g., the base model is split across multiple GPUs and we use tensor parallelism across them), then the combined memory capacity increases, allowing even more LoRA adapters to be packed into a single fine-tuning job.

**Packed LoRA fine-tuning workflow.** In LoRA fine-tuning with a single LoRA adapter [25], a single input is passed to both the base model and the LoRA adapter, and their outputs are merged with a scaling factor  $\alpha$  for the final output, as shown in Figure 1. In contrast, packed LoRA fine-tuning takes an array of multiple inputs with an input for each LoRA adapter, as shown in Figure 2. All inputs are passed to the base model and their corresponding LoRA adapters. The outputs from the base model and LoRA adapters are then merged. For example, suppose that the base model weight is  $W$  and two LoRA adapters, Adapter 1 with  $(A_1, B_1, \alpha_1)$  and Adapter 2 with  $(A_2, B_2, \alpha_2)$ , are packed into a LoRA fine-tuning job. The inputs of this fine-tuning job are  $X = [x_1, x_2]$  for the two adapters. Then the LoRA outputs of the two adapters are  $Y = [y_1, y_2]$ , where  $y_i = x_i(W + \alpha_i B_i \times A_i)$ . The computation of each adapter in packed LoRA fine-tuning is identical to LoRA fine-tuning with this single LoRA adapter.

Meanwhile, the base model is shared among LoRA adapters, offering opportunities for higher hardware utilization.

### 3.3 Challenges

Packing multiple LoRA adapters into a single fine-tuning job is analogous to increasing the batch size in LoRA fine-tuning. This approach improves hardware utilization and boosts the efficiency of LoRA hyperparameter tuning, but it also presents new challenges.

**How to efficiently support the computation of packed LoRA adapters on GPUs?** Packed LoRA fine-tuning consists of two components: the shared base model and the set of packed LoRA adapters. Since the base model is shared across all adapters, the input to its pretrained weight tensor is effectively the batched input from all packed adapters. However, since each LoRA adapter has its own input and weights, their computation cannot be merged directly. Naively iterating the computation of each LoRA adapter, as shown in Figure 2, will inevitably result in low hardware utilization in both forward propagation and backward propagation due to the small LoRA ranks and thus the low arithmetic intensity in the LoRA adapter.

**How to perform resource-aware packed LoRA scheduling?** Even with performant kernels for packed LoRA computation, effectively packing LoRA adapters into fine-tuning jobs remains challenging since the hardware cannot hold all the LoRA configurations, given the large hyperparameter search space. We need to determine how to pack LoRA adapters to maximize hardware utilization without causing OOM errors. In addition, since LoRA hyperparameter tuning typically involves multiple GPUs, e.g., eight GPUs in a single GPU instance from public GPU clouds [1–4], we also need to allocate hardware resources for each fine-tuning job. Maximizing fine-tuning throughput requires jointly optimizing both the packing of LoRA adapters and the allocation of compute resources; optimizing either in isolation is insufficient.

## 4 System Overview of PLoRA

We propose PLoRA, a system that enables efficient LoRA hyperparameter tuning with packed LoRA fine-tuning. Given the base model, the hardware pool, and a LoRA configuration search space, PLoRA optimizes LoRA hyperparameter tuning throughput by efficiently packing configurations to maximize hardware utilization. Figure 3 illustrates PLoRA’s architecture which consists of two major components: 1) a LoRA Execution Engine that launches packed LoRA fine-tuning jobs on hardware resources and optimizes the LoRA computations with Packed LoRA Kernels (§5), and 2) a LoRA Packing Planner that efficiently schedules LoRA configurations by jointly optimizing LoRA configuration packing and hardware allocation for fine-tuning jobs (§6).

PLoRA consists of two phases: offline LoRA configuration planning and online packed LoRA fine-tuning execution. We

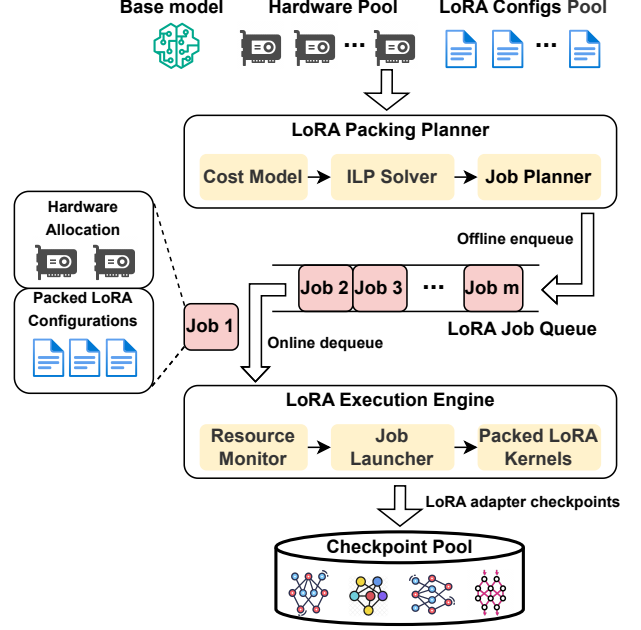


Figure 3. The system architecture of PLoRA.

define a *fine-tuning job* as a process that fine-tunes multiple packed LoRA adapters simultaneously on a shared copy of the base model. In the offline phase, PLoRA’s Packing Planner explores the search space of possible packed LoRA configurations to determine all fine-tuning jobs. It incorporates a cost model that estimates both memory usage and training throughput, using profiling data from the first few iterations (10 iterations in our testbed). Based on this cost model, the Job Planner decides how to pack LoRA adapters into fine-tuning jobs and allocates hardware resources by determining the appropriate degree of parallelism for each job. The resulting set of planned jobs is then enqueued in the LoRA Job Queue, serving as input to the Packed LoRA Engine for execution.

The LoRA Execution Engine then dynamically dequeues jobs from the LoRA Job Queue for online deployment based on the available hardware resources in the hardware pool, which is monitored by the Resource Monitor. Based on each job’s hardware allocation and packed LoRA configurations, the Job Launcher in the LoRA Execution Engine sets up the parallelism strategy and launches a corresponding packed fine-tuning job. Note that PLoRA will deploy multiple fine-tuning jobs concurrently, as long as the hardware pool has sufficient resources available. When running a packed LoRA fine-tuning job, the LoRA Execution Engine utilizes optimized GPU kernels for efficient LoRA computations during both forward and backward propagation, thereby improving hardware utilization.

Each LoRA adapter from the packed configurations is saved in the Checkpoint Pool at the end of a fine-tuning job. The hardware resources allocated to this job also become available for future fine-tuning jobs. The Resource Monitor



will be notified, and the Packed LoRA Engine then dequeues the next set of fine-tuning jobs from the LoRA Job Queue for execution on the available hardware.

## 5 Optimizing Packed LoRA Computation

### 5.1 Inefficient Computation in Existing Frameworks

LLM pre-training frameworks, such as Megatron-LM [44] and PyTorch [52], and LoRA fine-tuning frameworks, such as PEFT [37] and Unsloth [11], only support fine-tuning one configuration on a set of hardware at a time. Since LoRA adapters, when packed, share the same base model weights but have different adapter weights and inputs<sup>1</sup>, a naive approach to support fine-tuning with packed LoRA adapters is to batch the computation of the base model and sequentially compute each LoRA adapter (Figure 2). However, this approach results in poor fine-tuning throughput due to low hardware utilization when computing each LoRA adapter.

We profiled the fine-tuning performance using the naive approach as described above. We use Qwen-2.5-7B as the base model and apply a single LoRA adapter with batch size 1 on an A100 GPU as the baseline. The iteration time increases by 10% when the batch size is increased from 1 to 8. However, when we pack eight adapters into a fine-tuning job and each adapter has a batch size of 1, the naive approach worsens the iteration time by  $3.6\times$  compared to single LoRA tuning due to low hardware utilization in LoRA adapter computations. We also observe similar performance when fine-tuning Qwen-2.5-14B with two A100 GPUs and Qwen-2.5-32B with four A100 GPUs using TP. This confirms our hypothesis that the performance bottleneck is the sequential computation of LoRA adapters rather than the batched computation in the base model.

### 5.2 Packed LoRA Kernels

We devise custom CUDA kernels for PLoRA to efficiently batch the computation of LoRA adapters in both forward and backward propagations. We carefully tile the LoRA matrices and group gradient computations across multiple adapters to improve hardware utilization and handle load balancing for heterogeneous LoRA adapters.

Given a set of LoRA adapters, we concatenate the LoRA adapters into a tensor and design kernels which can compute forward and backward passes for all LoRA adapters. Our key insight in designing performant kernels is to tile the concatenated tensor along the sequence or hidden dimensions if possible. The sequence dimension consists of the input token sequence multiplied by the batch size. We avoid tiling along the LoRA rank dimension because the rank can be as small as 8, and sharding on the smaller dimension prevents GPUs from fully utilizing their compute resources.

<sup>1</sup>We replicate the input tokens for each LoRA adapter at the beginning of each fine-tuning iteration.

If we denote the dimension of LoRA A by  $(d, r)$  and the dimension of LoRA B by  $(r, k)$  (Figure 1), we typically have  $d \gg r$  and  $r \ll k$ . Previous work on serving multiple LoRA adapters [9] introduces a kernel that handles these two cases separately, by splitting the input dimension  $d$  for LoRA A and the output dimension  $k$  for LoRA B. While this is possible for the forward pass, backward propagation cannot simply reuse this strategy. When computing the activation gradients with respect to LoRA inputs, avoiding tiling over the rank dimension would require splitting the inner dimension for tiling. This strategy would require extra overhead in creating a scratch buffer for each tile, additional indices for bookkeeping, and extra synchronization and reduction steps for accumulating intermediate results, which would undermine the benefits of tiling over large dimensions.

In our work, we tackle the challenge of efficient backward propagation implementation and use the following strategy to obtain performant kernels.

**CUDA kernel design.** We built upon CUTLASS for our packed LoRA kernels. Four cases should be considered separately for the upstream weights and input gradients of LoRA A and LoRA B. Below, we outline our partitioning strategy for backpropagation in detail.

- Case 1, in which we compute the gradient for the weight of the LoRA B projection. We partition along the output dimension ( $k$ ) for the LoRA B projection matrix to ensure that the gradient computation correctly associates the  $i$ th LoRA’s slice with the corresponding input and output matrix slices. Tiling is done along the output dimension, and LoRA ranks  $r_1$  and  $r_2$  remain in each tile.

- Case 2, in which we compute the gradient for the input of the LoRA B projection. We tile over the sequence dimension and the LoRA rank dimension of the upstream gradient, and reduce over the input hidden dimension.

- Case 3, in which we compute the gradient for the weight of the LoRA A projection. We tile over the sequence dimension of input activations and the output dimension of the upstream gradients, using LoRA rank as the reduction axis.

- Case 4, in which we compute the gradient for the input of the LoRA A projection. We tile along the upstream gradients’ sequence and LoRA rank dimensions and use the concatenated LoRA rank dimension for reduction.

**Kernel performance tuning.** To achieve high kernel performance across different hardware setups, we tune the ThreadblockShape, WarpShape, and InstructionShape parameters in CUTLASS [45] to optimize performance. While the optimal settings vary depending on both the underlying hardware architecture and the GEMM problem dimensions, we simulate workloads using model dimensions from widely used 3B and 7B models, as well as sequence lengths ranging from 512 to 2048. We set the InstructionShape to (16, 8, 16) to match the tensor core instruction shape on Ampere GPUs. For WarpShape, we empirically found that (64, 64, 32) yields the best throughput on the A100, while (16, 64, 32) performs

best on the A10 without triggering memory errors. Based on these warp shapes, we configure ThreadblockShape as (128, 128, 32) on the A100 and (64, 64, 32) on A10 to ensure compatibility with WarpShape.

## 6 Scheduling of Packed LoRA Fine-tuning

This section describes how to schedule packed LoRA configurations for LoRA hyperparameter tuning. We first formalize the optimization problem by jointly considering LoRA configuration packing and hardware allocation for fine-tuning jobs. Since the formulation is NP-complete, we develop an approximate algorithm for this problem and analyze its performance.

### 6.1 Problem Formulation

The optimization goal is to minimize the *makespan* of training time for all configurations in the given search space on the specified hardware. We observe that the completion time of a LoRA fine-tuning job is mainly affected by two factors:

- **The packed LoRA configurations**, which determine the set of LoRA adapters fine-tuned in a job.
- **The degree of parallelism**, which determines the number of GPUs used for each fine-tuning job.

The optimization problem that minimizes the makespan  $t_{opt}$  can be formulated as follows:

$$\min t_{opt} \quad (1)$$

$$\text{s.t. } t_{opt} \geq s_j + T(\mathcal{H}_{j,k}, d_j), \quad \forall j \in J \quad (2)$$

$$\sum_{j \in J} \mathcal{H}_{jk} = 1, \quad \forall k \in K \quad (3)$$

$$s_{j'} \geq s_j + T(\mathcal{H}_{j,k}, d_j) - M(1 - \mathcal{W}_{jj'}) + \mathcal{Z}_{jj'}M, \quad (4)$$

$$\forall j \neq j', j, j' \in J$$

$$s_j \geq s_{j'} + T(\mathcal{H}_{j',k}, d_{j'}) - M(1 - \mathcal{W}_{jj'}) + \mathcal{Z}_{jj'}M, \quad (5)$$

$$\forall j \neq j', j, j' \in J$$

$$\mathcal{Z}_{jj'} + \mathcal{Z}_{j'j} = \mathcal{W}_{jj'}, \quad \forall j \neq j', j, j' \in J \quad (6)$$

$$\mathcal{W}_{jj'} \leq \mathcal{X}_{ij}, \mathcal{W}_{jj'} \leq \mathcal{X}_{i'j'}, \forall j \neq j', \forall i \quad (7)$$

$$\mathcal{W}_{jj'} \geq \mathcal{X}_{ij} + \mathcal{X}_{i'j'} - 1, \forall j \neq j', \forall i \quad (8)$$

$$\mathcal{X}_{ij}, \mathcal{H}_{jk} \in \{0, 1\}, \quad \forall i, \forall j \in J, \forall k \in K \quad (9)$$

$$\mathcal{Z}_{jj'}, \mathcal{W}_{jj'} \in \{0, 1\}, \quad \forall j \neq j', j, j' \in J \quad (10)$$

$$s_j \geq 0, \forall j \in J; \quad 1 \leq i \leq G \quad (11)$$

In this formulation, we input the number of hardware devices  $G$  and LoRA configurations  $K$ . The rest are variables that the optimization instances solve.  $J$  represents the set of jobs,  $\mathcal{X}_{ij}$  is a binary variable that equals 1 if job  $j$  is assigned to device  $i$ ,  $\mathcal{H}_{jk}$  is a binary parameter that indicates whether LoRA configuration  $k$  belongs to job  $j$ .  $s_j$  is the start time of job  $j$ ,  $\mathcal{Z}_{jj'}$  is a binary variable that ensures job ordering where  $\mathcal{Z}_{jj'} = 1$  if job  $j$  precedes job  $j'$  and does not overlap in time,  $\mathcal{W}_{jj'}$  is a binary variable indicating that whether job  $j$  and  $j'$  share at least one device. We employ  $M$  as an auxiliary

**Table 5.** Notation used in cost model formulation

Symbol	Description
<b>Model-related parameters</b>	
$C$	Memory load factor
$M_{\text{base}}$	Memory required for the base model
$M_{\text{lor},k}$	Memory required for LoRA configuration $k$
$M_{\text{gpu}}$	Total memory capacity of a GPU
$G$	Number of available GPU devices
$K$	Set of LoRA configurations
$J$	Set of training jobs
$M$	A large constant for scheduling ordering
$T()$	Duration of job, estimated with cost model
<b>Optimization variables</b>	
$\mathcal{X}_{ij}$	Binary variable: 1 if job $j$ runs on device $i$
$\mathcal{H}_{jk}$	Binary variable for LoRA assignment
$s_j$	Start time of job $j$
$r_k$	LoRA rank of LoRA configuration $k$
$\mathcal{Z}_{jj'}$	Binary variable for scheduling order
$\mathcal{W}_{jj'}$	Binary variable for device sharing
$d_j$	Number of GPUs used by job $j$

large constant in the ordering constraints [17]. During optimization for minimal makespan, the optimization instance would output how LoRA configurations are assigned to jobs ( $\mathcal{H}$ ), how jobs are assigned to devices ( $\mathcal{X}$ ), and when jobs are scheduled ( $\mathcal{Z}$ ).  $T()$  is the cost model used to estimate the training time of LoRA fine-tuning jobs; it is not a variable, but a function of the packed LoRA configurations  $\mathcal{H}_{j,k}$  and the parallelism degree  $d_j$ , where  $j$  is a job. The notations used in this section are listed in Table 5.

In our optimization setup, Equation (3) ensures that each LoRA configuration belongs to exactly one fine-tuning job; Inequalities (4), (5), and Equation (6) ensure that jobs sharing any devices do not overlap in time [41]; Inequalities (7) and (8) help enforce the prior constraint by setting  $\mathcal{W}_{jj'}$  to 1 when two jobs share at least one device [41]. The makespan is represented as the latest job completion timestamp in Inequality (2). Equations (9), (10), and (11) define the scope of the variables. This optimization problem also has constraints on GPU memory usage of each LoRA fine-tuning job and the number of GPUs that can be allocated to all concurrent jobs. We will discuss these constraints in §6.2.

This optimization problem is NP-complete as it can be viewed as a variant of a 0-1 knapsack problem [29]. In addition, our optimization formulation adds a new layer of complexity, as each job must first decide which LoRA configurations ( $\mathcal{H}_{jk}$ ) to train and determine the associated degree of parallelism.

### 6.2 An Approximate Solution

Since the total floating-point operations (FLOP) for LoRA adapters (without counting the FLOP of the base model),

called LoRA FLOP, is fixed given a hyperparameter search space, minimizing the makespan ( $t_{opt}$ ) to complete evaluating all LoRA configurations is equivalent to maximizing the average LoRA FLOP in this time frame. Therefore, we can convert the optimization problem discussed in §6.1 to a throughput format as

$$\max \frac{\sum_{k=1}^{|K|} FLOP_k}{t_{opt}}, \quad (12)$$

where  $FLOP_k$  represents the LoRA FLOP of configuration  $k$ .

While computing an optimal job schedule that maximizes average throughput remains challenging, we can instead focus on optimizing instantaneous throughput at the job level. This insight enables us to design a scheduling algorithm for the packed LoRA fine-tuning problem, with provable bounds on its performance relative to the optimal solution.

**Maximizing fine-tuning job throughput.** We define an optimization problem to maximize the instantaneous throughput of fine-tuning jobs given the number of GPUs,  $G$ , and a set of LoRA configurations,  $K$ . Note that we use LoRA rank in Eq (13) instead of LoRA FLOP by leveraging the linear scaling property of LoRA FLOP in rank (refer to §2.1).

$$\max \sum_{j=1}^m \frac{\sum_{k=1}^{|K|} \mathcal{H}_{j,k} * r_k}{T(\mathcal{H}_{j,k}, d_j)}, \quad (13)$$

$$\text{s.t. } M_{\text{base}} + \sum_{k=1}^{|K|} \mathcal{H}_{j,k} * M_{\text{lor},k} \leq C * M_{\text{gpu}} * d_j, \quad (14)$$

$$\forall 1 \leq j \leq m$$

$$\sum_j d_j \leq G, \quad 1 \leq j \leq m \quad (15)$$

$$1 \leq d_j \leq G, \quad d_j \in \{2^i \mid i \in \mathbb{N}\} \quad (16)$$

$$m \geq 1, \quad m \in \mathbb{Z} \quad (17)$$

where  $r_k$  represents the rank of LoRA configuration  $k$ ,  $m$  represents the number of jobs to be concurrently scheduled on the given hardware. In Inequality (14),  $M_{\text{base}}$  represents the memory cost of the base model,  $M_{\text{lor},k}$  represents the memory cost of fine-tuning LoRA adapter  $k$ ,  $M_{\text{gpu}}$  represents the memory capacity of the given GPU,  $d_j$  represents the parallelism degree associated with job  $j$ , and  $C \in (0, 1]$  represents a user-specified memory load factor. Inequality (14) ensures that the packed LoRA configurations do not exceed hardware memory limits. Inequality (15) ensures that concurrent fine-tuning jobs do not use more GPUs than are available. Inequalities (16) and (17) define the ranges for the listed constants and variables. In this way, we approximate minimizing the LoRA training makespan by maximizing the LoRA fine-tuning throughput.

**ILP Solvable with determined parallelism degree.** We note that maximizing the packed LoRA fine-tuning throughput is still nonconvex because the denominator  $T(\mathcal{H}_{j,k}, d_j)$  depends on the variable  $d_j$ . While the solver cannot directly

---

**Algorithm 1:** Decomposed Throughput Maximization (DTM)

---

**Input:** Number of GPUs  $G$ , LoRA configuration space  $K$   
**Output:** Scheduling policy, which is a set of packed LoRA configurations and their parallelism degrees.

---

```

1 def DTMHelper( $g, P_{tmp}, K, P$ ):
2     if  $g \leq 0$  or  $K = \emptyset$  then
3          $P \leftarrow P \cup P_{tmp}$ ;
4         return;
5      $g' \leftarrow 2^{\lfloor \log_2 g \rfloor}$ ; // Round down
6     //  $d$  represents parallelism degree
7     foreach  $d \in \{g', g'/2, \dots, 1\}$  do
8         // Call Gurobi ILP solver
9          $P_{new}, K_{used} \leftarrow F(d, K)$ ;
10        DTMHelper( $g - d, P_{tmp} \cup P_{new}, K - K_{used}$ );
11
12 def DTM( $G, K$ ):
13      $P \leftarrow \emptyset$ ;
14     DTMHelper( $G, \emptyset, K, P$ );
15     return arg min  $\{T(p) \mid p \in P\}$ ;

```

---

optimize the instantaneous throughput, we observe that the parallelization degrees are powers of 2, making it feasible to enumerate the denominator. Therefore, we design an ILP solvable optimization problem with the parallelism degree equal to the given number of GPUs, i.e., only one packed LoRA fine-tuning job is determined.

$$F(D, K) = \frac{\sum_{k=1}^{|K|} \mathcal{H}_k * r_k}{T(\mathcal{H}_k, D)}, \quad (18)$$

$$\text{s.t. } M_{\text{base}} + \sum_{k=1}^{|K|} \mathcal{H}_k * M_{\text{lor},k} \leq C * M_{\text{gpu}} * D, \quad (19)$$

where  $\mathcal{H}_k$  is a binary parameter that indicates whether LoRA configuration  $k$  belongs to the job.

Based on Expression (18), we formulate the problem of maximizing fine-tuning job throughput and solve it using a recursive DTM algorithm, as shown in Algorithm 1. The algorithm begins by invoking the solver to optimize the throughput function  $F(D, K)$  under various degrees of parallelism (Line 5). It then recursively solves the resulting subproblems using an ILP solver to finish the enumeration process (Lines 6–7). DTMHelper() terminates and returns the current scheduling policy when either 1) no GPUs remain available, or 2) all LoRA configurations have been scheduled. We store all scheduling policies in  $P$  (Line 3). Finally, the algorithm selects and returns the scheduling policy that yields the minimum makespan (Line 11).

**The job planner.** Algorithm 1 finds the best LoRA packing scheduling policy that maximizes concurrent throughput of fine-tuning jobs on a set of available hardware. We then



**Algorithm 2:** The Job Planner**Input:** Number of GPUs  $G$ , LoRA configuration space  $K$ **Output:** LoRA job queue  $Q$ 


---

```

1  $Q \leftarrow []$ ;
2 Initialize available GPUs  $g_{avail} \leftarrow G$ ;
3 while  $K \neq \emptyset$  do
4   if  $g_{avail} > 0$  then
5      $P \leftarrow \text{DTM}(g_{avail}, K)$ ;
6     foreach  $p \in P$  do
7        $K \leftarrow K - p.\text{configs}$ ;    // Update configs
8      $Q.\text{append}(P)$ ;
9   Predict next job completion event and update  $g_{avail}$ ;
10 return  $Q$ ;
```

---

schedule all LoRA configurations from a search space to approximately solve Problem (12), which is equivalent to the makespan optimization problem, by considering the order in which LoRA fine-tuning jobs run on the given hardware resources. The core principle for the job planner is to schedule packed LoRA fine-tuning jobs with the maximum concurrent throughput whenever hardware resources are available.

The job planning algorithm is listed in Algorithm 2. If there are available GPU resources for job scheduling (Line 4), it invokes  $\text{DTM}()$  introduced in Algorithm 1 to find the best set of packed LoRA fine-tuning jobs for these available resources (Line 5) and updates the remaining LoRA configurations (Line 7). The job planner also adds the set of jobs into the LoRA job queue (Line 8). It then predicts the next job completion event with the cost model and updates the number of available GPUs for the next round of job planning.

**Computation time of the job planner.** The running time of the job planner is negligible, especially considering this is for offline scheduling. Suppose there are eight GPUs available as hardware resources for LoRA hyperparameter tuning, the ILP solver will be called 286 times in each  $\text{DTM}()$ . Since solving each optimization instance takes less than a second and all recursive branches can be performed in parallel, we observe that the computation time of Algorithm 1 is within 10 minutes in our evaluation with 120 configurations (§7.2). **Algorithm analysis.** Algorithm 2 performs optimally in a streaming setting with an unlimited number of jobs, as it consistently selects the job with the highest concurrent LoRA fine-tuning throughput. However, in our setting with a finite number of jobs, this approach can lead to a tail effect: the final jobs may not fully utilize all available hardware resources, resulting in suboptimal overall throughput compared to the optimal solution. We now bound this tail effect.

**Theorem 6.1** (Bounded Tail Effect with Algo 2). *Let  $J$  be a set of jobs scheduled on  $G$  GPUs. Let  $j \in J$  be the last job that uses  $D$  GPUs. Let  $T_{last}$  be the fine-tuning time of the last job and  $F$  be the makespan based on the job planner’s schedule.*

*Then, the approximation ratio (AR) of the job planner for the makespan optimization problem is upper bounded by:*

$$AR \leq \frac{F}{F - T_{last} \cdot \frac{G-D}{G}}.$$

See Appendix C for the detailed proof. In practice, using experiment settings from §7, we calculate the approximation ratio (AR) and find that PLoRA produces schedules with AR between 1.05 and 1.14.

## 7 Evaluation

In this section, we will demonstrate the effectiveness of PLoRA for LoRA hyperparameter tuning. Specifically, we will address the following questions:

- **Efficient hyperparameter tuning:** Can PLoRA reduce the makespan of LoRA hyperparameter tuning? (§7.2)
- **Model quality:** Does PLoRA find better LoRA adapters that improve model quality? (§7.3)
- **Ablation study:** How do PLoRA’s individual components perform? (§7.4)
- **Generality:** How is PLoRA’s performance on different hardware architectures? (§7.5)

### 7.1 Experiment Setup

**Testbed.** We conduct experiments with a G5 and a P4d 24xlarge instance from Amazon EC2. The P4d instance has 8 A100 GPUs (40 GB) connected by NVLink for GPU-to-GPU communication. The G5 instance has 8 A10 GPUs (24 GB) connected by PCIe Gen4 for GPU-to-GPU communication.

**Models and tasks.** We conduct experiments on the Qwen 2.5 model family, one of the frontier open-weight model families that provides the most complete model size selections, including, but not limited to 3B, 7B, 14B, and 32B. We also evaluate PLoRA with LLAMA-3.2-3B and LLAMA-3.1-8B. We perform our evaluation in a zero-shot setting, following the prompting template in prior work [51]. We use four downstream tasks, GSM8K [10], mrpc [47], cola [47], and wnli [47] and set sequence length as 1024.

**LoRA configuration selection.** In LoRA hyperparameter tuning, the search space is specified by users. The search space in our evaluations consists of four knobs: learning rate, batch size, LoRA rank, and LoRA alpha. Their ranges are listed in Table 1. We select a total of 120 LoRA configurations for the experiments.

**Baselines.** We compare PLoRA with sequential approaches for LoRA hyperparameter tuning, in which each LoRA fine-tuning job only evaluates one LoRA adapter. We consider two strategies for sequential approaches: *Min GPU*, which uses the minimum set of hardware that satisfies the memory constraints for each LoRA fine-tuning job and launches parallel jobs to fill all GPUs; and *Max GPU*, which uses the maximum number of devices within a GPU instance for each LoRA fine-tuning job, i.e., TP degree is 8 for all evaluated

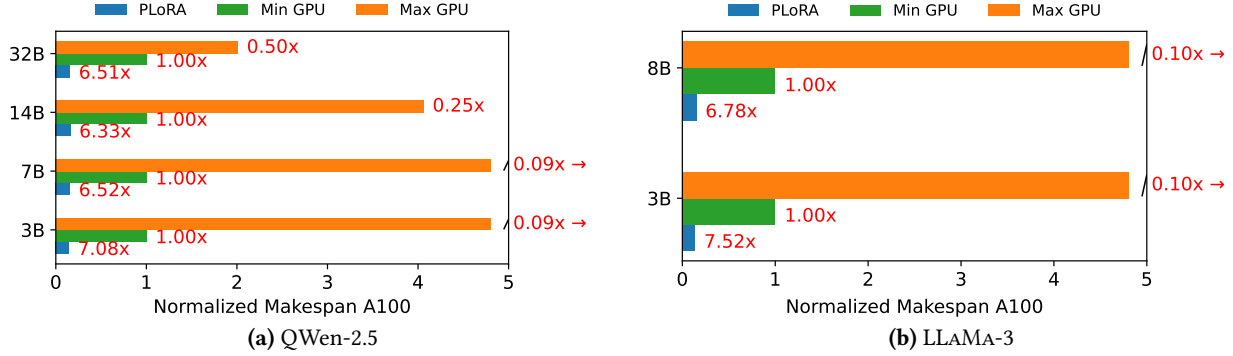


**Figure 4.** The makespan of LoRA hyperparameter tuning with different methods on A100 GPUs. The makespan is normalized to the performance of Min GPU.

models in our testbed. While we evaluate it with tensor parallelism, we believe the proposed design is also applicable to other parallelisms, such as pipeline parallelism [38] and FSDP [52], which are part of our future work.

**Metrics.** We use the makespan to evaluate the end-to-end performance of LoRA hyperparameter tuning, which evaluates all LoRA configurations in the search space. We use throughput to evaluate the performance of LoRA fine-tuning jobs and packed LoRA kernels. We report the zero-shot accuracy on the downstream tasks.

**Implementation.** We implement a prototype of PLoRA atop torchtune [46]. Our implementation contains around 5000 lines of Python code and around 800 lines of code in a CUTLASS-based CUDA implementation for customized packed LoRA kernels. We use cvxpy [13] to implement our optimization module and built upon the PyTorch DTensor primitive to customize LoRA tensor parallel sharding strategies for efficient fine-tuning with tensor parallelism.

## 7.2 Fine-tuning Throughput on A100 GPUs

**7.2.1 Makespan evaluation.** We evaluate the makespan improvement of PLoRA over the two baselines by running 120 LoRA configurations from the search space. We begin with the QWen-2.5 family as the base models. Since a single GPU can accommodate the 3B and 7B variants, but the 14B requires two GPUs and 32B models require four GPUs, the TP degrees in Min GPU and Max GPU are as follows. Min GPU: 1) for the 3B and 7B models, each LoRA fine-tuning job runs on a single GPU, allowing eight concurrent jobs; 2) for the 14B model, each job utilizes two GPUs, allowing for a total of four concurrent jobs; 3) and for the 32B model, each job utilizes four GPUs, allowing for two concurrent jobs. Max GPU: Each LoRA fine-tuning job uses all eight GPUs, allowing only one job to run at a time.

Figure 4a shows the makespan normalized to Min GPU. The performance of Max GPU is much worse than that of Min GPU due to even lower hardware utilization. On the contrary, PLoRA reduces the makespan by 6.51× and 6.33×

on 14B and 32B, respectively, thanks to packed LoRA fine-tuning. PLoRA also achieves 7.08× and 6.52× reduction in makespan on the 3B and 7B models.

We also evaluate LLAMA-3.2-3B and LLAMA-3.1-8B as the base models and observe similar improvements in makespan. Min GPU runs each LoRA fine-tuning job with one GPU, and eight concurrent jobs are launched. Max GPU still has the worst makespan, as shown in Figure 4b. PLoRA achieves 7.52× speedups over Min GPU for LLAMA-3.2-3B and 6.78× speedup for LLAMA-3.1-8B.

**7.2.2 Job-level throughput evaluation.** We study the benefits of packing by measuring the throughput of packed LoRA fine-tuning jobs compared to our baselines. We run PLoRA with different base models and batch sizes on A100 GPUs. We fix LoRA rank to be 32 and other settings of PLoRA, Min GPU, and Max GPU are the same as those in §7.2.1. We show the job throughput on QWen-2.5 models in Figure 5. We observe similar trends in the LLAMA-3 models.

For a batch size of 1, PLoRA achieves up to 12.8× speedup across the tested models. When we increase the batch size, the performance gain reduces since the Min GPU strategy can better utilize the hardware. However, the table shows that we still achieve a significant throughput improvement for a batch size of 4. Further increasing batch sizes harms model quality, as discussed in §3.

## 7.3 Model quality with PLoRA

In this section, we evaluate the model quality of the best LoRA adapter found by PLoRA from the given search space with 120 LoRA configurations. Four base models, QWen-2.5-3B, QWen-2.5-7B, LLAMA-3.2-3B, and LLAMA-3.1-8B are fine-tuned with LoRA on four downstream tasks.

The model quality is listed in Table 6. The first number in each cell is the model quality of the base model without LoRA fine-tuning. The second number in each cell is the model quality of the LoRA adapter fine-tuned with the default hyperparameters from Unsloth [11], one of the most popular LoRA fine-tuning frameworks. The third number is

## PLoRA

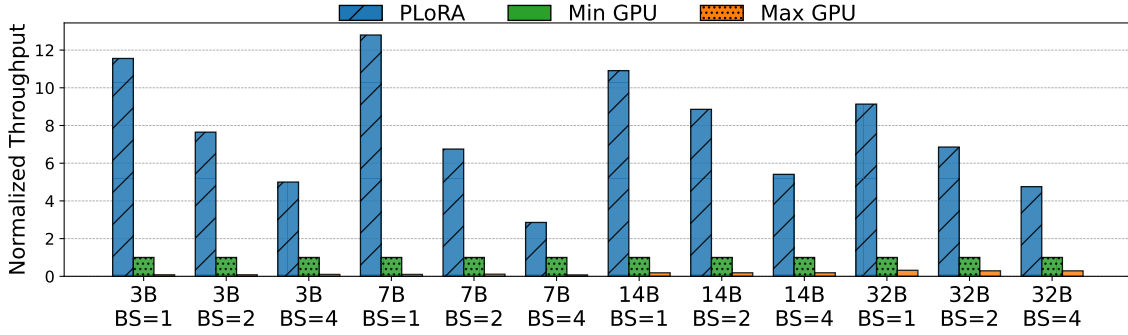


**Figure 5.** LoRA fine-tuning job throughput for various Qwen-2.5 model sizes and batch sizes (BS) on A100 GPUs. The performance is normalized to Min GPU.

**Table 6.** Model quality comparison of different models with no LoRA, the default LoRA configuration, and the best LoRA configuration. The first number in each cell is the quality of the base model, the second is for the default configuration, and the third is for the best configuration. The fourth number is the quality improvement with the best LoRA configuration over the default one.

	QWen-2.5-3B			QWen-2.5-7B			LLAMA-3.2-3B			LLAMA-3.1-8B		
mrpc	62.4	62.6	67.6	+5.0%	64.1	64.7	70.0	+5.3%	70.3	77.4	80.6	+3.2%
cola	48.8	53.8	77.2	+23.4%	62.7	68.4	80.2	+11.8%	69.9	71.8	77.3	+5.5%
wnli	53.5	66.2	73.4	+7.2%	78.8	80.1	84.5	+4.4%	46.4	61.9	64.8	+2.9%
gsm8k	61.2	64.8	74.6	+9.8%	70.8	72.1	79.8	+7.7%	60.4	63.3	71.3	+8.0%
									69.6	70.5	78.0	+7.5%

**Table 7.** The normalized throughput improvement of packed LoRA kernels over sequential LoRA computations. The first number in each cell represents the throughput speedup in the forward pass, while the second number represents that in the backward pass.

Num. LoRA	3B Attention d = 2048	3B MLP 11008	7B Attention 3584	7B MLP 18944
2	2.00x/2.01x	1.98x / 1.98x	1.90x/1.92x	1.99x / 1.99x
8	7.98x/7.96x	7.60x / 7.67x	7.51x/7.92x	7.77x / 7.80x
32	29.0x/30.0x	26.5x / 26.9x	26.7x/31.2x	28.4x / 28.7x

the model quality of the best LoRA adapter from the search space. We also list the model quality improvement (the fourth number in red) of the best configuration compared to the default one. We can see from the table that the default set of hyperparameters allows LoRA to achieve better model quality on downstream tasks than the base model. However, it does not fully fulfill LoRA’s potential for fine-tuning. After searching 120 LoRA configurations with PLoRA, the best LoRA adapters significantly outperform those with the default LoRA configuration by up to 23.4%. These results also hold across different model families.

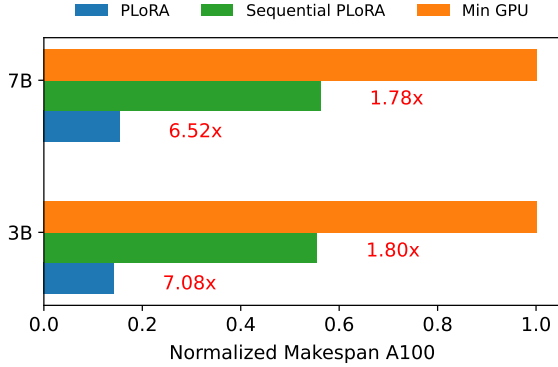
## 7.4 Microbenchmarks

**7.4.1 Packed LoRA kernel performance.** We examine the performance of our customized LoRA kernels in various workloads on A100 GPUs. Consider a LoRA tensor with

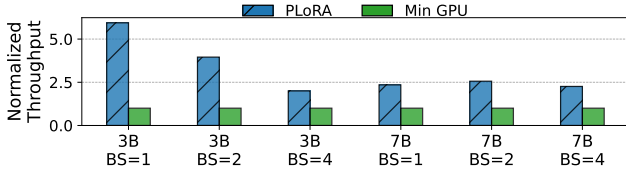
a shape  $[r, d]$ , where  $r$  is the LoRA rank and  $d$  is the hidden dimension in the base model. We vary both  $r$  and  $d$  to evaluate the computational efficiency of the packed LoRA kernel. We first fix  $r = 64$ , set  $d$  to different values based on the hidden dimensions in the Attention and MLP layers of QWen-2.5-3B and QWen-2.5-7B, and set the batch size to 1. We pack different numbers of LoRA computations into a kernel (ranging from 2 to 32) and compare the forward and backward computation performance with a sequential baseline.

Table 7 reports the throughput improvement normalized to the performance of the baseline. As we increase the number of packed LoRA computations from 2 to 32, our packed LoRA kernels exhibit close to linear speedups over the baseline in both forward and backward propagation. This trend holds for a wide range of hidden dimensions, from 2048 to 18944, as well as LoRA ranks, from 8 to 128. More performance results on A10 GPUs can be found in Appendix B.1.

**7.4.2 Speedup breakdown.** PLoRA’s performance gains mainly come from two components: optimized GPU kernels for efficient packed LoRA computations and near-optimal scheduling for packing LoRA configurations. This ablation study breaks down how each component contributes to the overall reduction in makespan. We compare the makespan of LoRA hyperparameter tuning with Min GPU, using PLoRA for job planning but executing LoRA sequentially (Sequential PLoRA), and PLoRA. The results normalized to Min GPU



**Figure 6.** This figure shows the breakdown of PLoRA’s speedup on A100 GPUs. Sequential PLoRA represents the speedup obtained via leveraging PLoRA’s Packing Planner, but performs vanilla sequential LoRA training without PLoRA’s Execution Engine.



**Figure 7.** This figure shows the LoRA fine-tuning throughput for various models and batch sizes on A10 GPUs normalized to the Min GPU baseline.

are shown in Figure 6. We use QWen-2.5-3B and QWen-2.5-7B as base models and use a search space consisting of 120 LoRA configurations. Sequential PLoRA reduces the makespan by around 1.8 $\times$  for both models via amortizing the base model computation. The optimized GPU kernels further reduce the makespan by up to 3.93 $\times$ , demonstrating that both components contribute significantly to PLoRA’s performance.

### 7.5 Fine-tuning Throughput on A10 GPUs

We evaluate PLoRA on A10 GPUs using the QWen-2.5-3B and QWen-2.5-7B models, with a LoRA rank of 32. The throughput of LoRA fine-tuning jobs is shown in Figure 7, and the performance is normalized to the Min GPU baseline. PLoRA achieves 5.94 $\times$  speedup for 3B and 2.56 $\times$  speedup for 7B. The throughput improvement is lower than that on A100 GPUs, which is expected because A10 GPUs have less GPU memory capacity than A100 GPUs and, therefore, can pack fewer LoRA adapters in LoRA fine-tuning jobs.

We also evaluate PLoRA on base models with QLoRA [12], which quantizes the weights of the base model to 4 bits. QLoRA reduces the GPU memory usage of the base model, leaving more memory for LoRA adapters. We enable QLoRA

in PLoRA and evaluate the performance with QWen-2.5-7B. We use LoRA with a rank of 32 and a batch size of 1 in all LoRA configurations. PLoRA achieves 4.72 $\times$  speedup compared to standard QLoRA fine-tuning with a single LoRA. This experiment shows that quantization, an orthogonal approach to boost LoRA fine-tuning efficiency, can work with PLoRA to further improve fine-tuning throughput by packing more LoRA adapters in LoRA fine-tuning jobs.

## 8 Related works

**LoRA-related systems.** Efficient LoRA serving has been extensively studied. DLoRA [48] develops scheduling algorithms for efficient multi-LoRA serving. Punica [9] designs optimized GPU kernels for batched LoRA inference, and SLoRA [43] proposes memory management to support thousands of LoRA adapters for multi-LoRA serving. However, these systems focus on LoRA serving and assume that LoRA adapters have been well-trained. In contrast, PLoRA optimizes the system efficiency of LoRA hyperparameter tuning to find the best LoRA adapter from a search space.

**Hyperparameter tuning.** Hyperparameter tuning has been well-studied for model pretraining and other workloads. Existing techniques, such as grid search [6], random search [7], and Bayesian optimization [28], are designed to reduce the search space, which is orthogonal to our study. PLoRA can work with different hyperparameter tuning algorithms based on the configuration space provided to the planner (e.g., the entire space for grid search [6] or a chosen set in case of asynchronous Bayesian optimization [27]). Many hyperparameter tuning systems have also been proposed for model pretraining, including Seer [15], KungFu [36], Optuna [5], AutoWEKA [30], and ASHA [32]. However, these techniques and systems cannot address the issues of low hardware utilization when fine-tuning a single LoRA configuration. Our work focuses on efficient LoRA hyperparameter tuning and leveraging underutilized hardware resources to sweep the hyperparameter search space. To the best of our knowledge, we are the first work to tackle the challenges of LoRA hyperparameter tuning via efficient hyperparameter sweep with packed LoRA fine-tuning. We note that these orthogonal hyperparameter tuning methods can be applied on top of our system to unlock further efficiency gains.

**Job scheduling.** Makespan minimization is an extensively studied topic in generalized cluster job scheduling [18, 39, 49]. In the cluster scheduling setup, hardware resources serve as a hyperparameter that the user inputs, but the challenge is to optimize for job completion time [21, 26] and makespan [39] or ensuring fairness [8, 19, 35]. Recently, Gavel [39] has extended this to a heterogeneous hardware setting. These prior works on generalized cluster scheduling assume jobs are predefined. However, in LoRA hyperparameter tuning, PLoRA’s optimization module also determines how LoRA configurations are packed into each job and their degree

of parallelism. We leverage additional information about LoRA configurations and hardware resources to optimize job scheduling and joint allocation of GPU resources.

## 9 Conclusion

This paper presents PLoRA, a system for efficiently tuning LoRA hyperparameters. We conduct an extensive empirical study to demonstrate the need for LoRA hyperparameter tuning and identify inefficiencies in current tuning pipelines. We leverage these insights to design a LoRA packing planner and an execution engine and build a parallel LoRA fine-tuning framework. PLoRA improves the fine-tuning throughput by up to 12.8 $\times$  over traditional approaches by packing multiple LoRA adapters in a fine-tuning job and reduces makespan by up to 7.52 $\times$  across tested models.

## References

- [1] 2023. GPU instances in Google Cloud Platform. <https://cloud.google.com/compute/docs/gpus>.
- [2] 2023. ND40rs\_v2 in Azure. <https://learn.microsoft.com/en-us/azure/virtual-machines/ndv2-series>.
- [3] 2023. ND96asr\_v4 in Azure. <https://learn.microsoft.com/en-us/azure/virtual-machines/nda100-v4-series>.
- [4] 2023. P4d.24xlarge in AWS. <https://aws.amazon.com/ec2/instance-types/p4/>.
- [5] Takuya Akiba, Shotaro Sano, Toshihiko Yanase, Takeru Ohta, and Masanori Koyama. 2019. Optuna: A next-generation hyperparameter optimization framework. In *Proceedings of the 25th ACM SIGKDD international conference on knowledge discovery & data mining*. 2623–2631.
- [6] James Bergstra, Rémi Bardenet, Yoshua Bengio, and Balázs Kégl. 2011. Algorithms for hyper-parameter optimization. *Advances in neural information processing systems* 24 (2011).
- [7] James Bergstra and Yoshua Bengio. 2012. Random search for hyper-parameter optimization. *The journal of machine learning research* 13, 1 (2012), 281–305.
- [8] Shubham Chaudhary, Ramachandran Ramjee, Muthian Sivathanu, Nipun Kwatra, and Srinidhi Viswanatha. 2020. Balancing efficiency and fairness in heterogeneous GPU clusters for deep learning. In *Proceedings of the Fifteenth European Conference on Computer Systems*. 1–16.
- [9] Lequn Chen, Zihao Ye, Yongji Wu, Danyang Zhuo, Luis Ceze, and Arvind Krishnamurthy. 2024. Punica: Multi-tenant lora serving. *Proceedings of Machine Learning and Systems* 6 (2024), 1–13.
- [10] Karl Cobbe, Vineet Kosaraju, Mohammad Bavarian, Mark Chen, Heewoo Jun, Lukasz Kaiser, Matthias Plappert, Jerry Tworek, Jacob Hilton, Reiichiro Nakano, et al. 2021. Training verifiers to solve math word problems. *arXiv preprint arXiv:2110.14168* (2021).
- [11] Michael Han Daniel Han and Unsloth team. 2023. *Unsloth*. <http://github.com/unslothai/unsloth>
- [12] Tim Dettmers, Artidoro Pagnoni, Ari Holtzman, and Luke Zettlemoyer. 2023. Qlora: Efficient finetuning of quantized llms. *Advances in neural information processing systems* 36 (2023), 10088–10115.
- [13] Steven Diamond and Stephen Boyd. 2016. CVXPY: A Python-embedded modeling language for convex optimization. *Journal of Machine Learning Research* 17, 83 (2016), 1–5.
- [14] Ning Ding, Yujia Qin, Guang Yang, Fuchao Wei, Zonghan Yang, Yusheng Su, Shengding Hu, Yulin Chen, Chi-Min Chan, Weize Chen, et al. 2023. Parameter-efficient fine-tuning of large-scale pre-trained language models. *Nature Machine Intelligence* 5, 3 (2023), 220–235.
- [15] Lisa Dunlap, Kirthivasan Kandasamy, Ujval Misra, Richard Liaw, Michael Jordan, Ion Stoica, and Joseph E Gonzalez. 2021. Elastic hyperparameter tuning on the cloud. In *Proceedings of the ACM Symposium on Cloud Computing*. 33–46.
- [16] Vlad Fomenko, Han Yu, Jongho Lee, Stanley Hsieh, and Weizhu Chen. 2024. A Note on LoRA. *arXiv preprint arXiv:2404.05086* (2024).
- [17] Marco Ghirardi and Chris N Potts. 2005. Makespan minimization for scheduling unrelated parallel machines: A recovering beam search approach. *European Journal of Operational Research* 165, 2 (2005), 457–467.
- [18] Robert Grandl, Ganesh Ananthanarayanan, Srikanth Kandula, Sriram Rao, and Aditya Akella. 2014. Multi-resource packing for cluster schedulers. *ACM SIGCOMM Computer Communication Review* 44, 4 (2014), 455–466.
- [19] Robert Grandl, Srikanth Kandula, Sriram Rao, Aditya Akella, and Janardhan Kulkarni. 2016. {GRAPHENE}: Packing and {Dependency-Aware} scheduling for {Data-Parallel} clusters. In *12th USENIX Symposium on Operating Systems Design and Implementation (OSDI 16)*. 81–97.
- [20] Aaron Grattafiori, Abhimanyu Dubey, Abhinav Jauhri, Abhinav Pandey, Abhishek Kadian, Ahmad Al-Dahle, Aiesha Letman, Akhil Mathur, Alan Schelten, Alex Vaughan, et al. 2024. The llama 3 herd of models. *arXiv preprint arXiv:2407.21783* (2024).
- [21] Juncheng Gu, Mosharaf Chowdhury, Kang G Shin, Yibo Zhu, Myeongjae Jeon, Junjie Qian, Hongqiang Liu, and Chuanxiong Guo. 2019. Tiresias: A {GPU} cluster manager for distributed deep learning. In *16th USENIX Symposium on Networked Systems Design and Implementation (NSDI 19)*. 485–500.
- [22] Tom Gunter, Zirui Wang, Chong Wang, Ruoming Pang, Andy Narayanan, Aonan Zhang, Bowen Zhang, Chen Chen, Chung-Cheng Chiu, David Qiu, et al. 2024. Apple intelligence foundation language models. *arXiv preprint arXiv:2407.21075* (2024).
- [23] Daya Guo, Dejian Yang, Haowei Zhang, Junxiao Song, Ruoyu Zhang, Runxin Xu, Qihao Zhu, Shirong Ma, Peiyi Wang, Xiao Bi, et al. 2025. Deepseek-r1: Incentivizing reasoning capability in llms via reinforcement learning. *arXiv preprint arXiv:2501.12948* (2025).
- [24] Jeremy Howard and Sebastian Ruder. 2018. Universal language model fine-tuning for text classification. *arXiv preprint arXiv:1801.06146* (2018).
- [25] Edward J Hu, Yelong Shen, Phillip Wallis, Zeyuan Allen-Zhu, Yuanzhi Li, Shean Wang, Lu Wang, and Weizhu Chen. 2021. Lora: Low-rank adaptation of large language models. *arXiv preprint arXiv:2106.09685* (2021).
- [26] Qinghao Hu, Peng Sun, Shengen Yan, Yonggang Wen, and Tianwei Zhang. 2021. Characterization and prediction of deep learning workloads in large-scale gpu datacenters. In *Proceedings of the International Conference for High Performance Computing, Networking, Storage and Analysis*. 1–15.
- [27] Kirthivasan Kandasamy, Akshay Krishnamurthy, Jeff Schneider, and Barnabas Poczos. 2017. Asynchronous parallel Bayesian optimisation via Thompson sampling. *arXiv preprint arXiv:1705.09236* (2017).
- [28] Kirthivasan Kandasamy, Karun Raju Vysyaraju, Willie Neiswanger, Biswajit Paria, Christopher R Collins, Jeff Schneider, Barnabas Poczos, and Eric P Xing. 2020. Tuning hyperparameters without grad students: Scalable and robust bayesian optimisation with dragonfly. *Journal of Machine Learning Research* 21, 81 (2020), 1–27.
- [29] Richard M Karp. 2009. Reducibility among combinatorial problems. In *50 Years of Integer Programming 1958-2008: from the Early Years to the State-of-the-Art*. Springer, 219–241.
- [30] Lars Kotthoff, Chris Thornton, Holger H Hoos, Frank Hutter, and Kevin Leyton-Brown. 2017. Auto-WEKA 2.0: Automatic model selection and hyperparameter optimization in WEKA. *Journal of Machine Learning Research* 18, 25 (2017), 1–5.

- [31] Woosuk Kwon, Zhuohan Li, Siyuan Zhuang, Ying Sheng, Lianmin Zheng, Cody Hao Yu, Joseph Gonzalez, Hao Zhang, and Ion Stoica. 2023. Efficient memory management for large language model serving with pagedattention. In *Proceedings of the 29th Symposium on Operating Systems Principles*. 611–626.
- [32] Liam Li, Kevin Jamieson, Afshin Rostamizadeh, Ekaterina Gonina, Jonathan Ben-Tzur, Moritz Hardt, Benjamin Recht, and Ameet Talwalkar. 2020. A system for massively parallel hyperparameter tuning. *Proceedings of machine learning and systems 2* (2020), 230–246.
- [33] Zhimin Li, Jianwei Zhang, Qin Lin, Jiangfeng Xiong, Yanxin Long, Xincheng Deng, Yingfang Zhang, Xingchao Liu, Minbin Huang, Zedong Xiao, Dayou Chen, Jiajun He, Jiahao Li, Wenyue Li, Chen Zhang, Rongwei Quan, Jianxiang Lu, Jiabin Huang, Xiaoyan Yuan, Xiaoxiao Zheng, Yixuan Li, Jihong Zhang, Chao Zhang, Meng Chen, Jie Liu, Zheng Fang, Weiyan Wang, Jinbao Xue, Yangyu Tao, Jianchen Zhu, Kai Liu, Sihuan Lin, Yifu Sun, Yun Li, Dongdong Wang, Mingtao Chen, Zhichao Hu, Xiao Xiao, Yan Chen, Yuhong Liu, Wei Liu, Di Wang, Yong Yang, Jie Jiang, and Qinglin Lu. 2024. Hunyuan-DiT: A Powerful Multi-Resolution Diffusion Transformer with Fine-Grained Chinese Understanding. *arXiv:2405.08748 [cs.CV]*
- [34] Haotian Liu, Chunyuan Li, Qingyang Wu, and Yong Jae Lee. 2023. Visual instruction tuning. *Advances in neural information processing systems 36* (2023), 34892–34916.
- [35] Kshiteej Mahajan, Arjun Balasubramanian, Arjun Singhvi, Shivaram Venkataraman, Aditya Akella, Amar Phanishayee, and Shuchi Chawla. 2020. Themis: Fair and efficient {GPU} cluster scheduling. In *17th USENIX Symposium on Networked Systems Design and Implementation (NSDI 20)*. 289–304.
- [36] Luo Mai, Guo Li, Marcel Wagenländer, Konstantinos Fertakis, Andrei-Octavian Brabete, and Peter Pietzuch. 2020. {KungFu}: Making training in distributed machine learning adaptive. In *14th USENIX Symposium on Operating Systems Design and Implementation (OSDI 20)*. 937–954.
- [37] Sourab Mangrulkar, Sylvain Gugger, Lysandre Debut, Younes Belkada, Sayak Paul, and Benjamin Bossan. 2022. PEFT: State-of-the-art Parameter-Efficient Fine-Tuning methods. <https://github.com/huggingface/peft>.
- [38] Deepak Narayanan, Aaron Harlap, Amar Phanishayee, Vivek Seshadri, Nikhil R Devanur, Gregory R Ganger, Phillip B Gibbons, and Matei Zaharia. 2019. PipeDream: Generalized pipeline parallelism for DNN training. In *Proceedings of the 27th ACM symposium on operating systems principles*. 1–15.
- [39] Deepak Narayanan, Keshav Santhanam, Fiodar Kazhemiaka, Amar Phanishayee, and Matei Zaharia. 2020. {Heterogeneity-Aware} cluster scheduling policies for deep learning workloads. In *14th USENIX Symposium on Operating Systems Design and Implementation (OSDI 20)*. 481–498.
- [40] Long Ouyang, Jeffrey Wu, Xu Jiang, Diogo Almeida, Carroll Wainwright, Pamela Mishkin, Chong Zhang, Sandhini Agarwal, Katarina Slama, Alex Ray, et al. 2022. Training language models to follow instructions with human feedback. *Advances in neural information processing systems 35* (2022), 27730–27744.
- [41] Michael L. Pinedo. 2008. *Scheduling: Theory, Algorithms, and Systems* (3rd ed.). Springer Publishing Company, Incorporated.
- [42] Robin Rombach, Andreas Blattmann, Dominik Lorenz, Patrick Esser, and Björn Ommer. 2021. High-Resolution Image Synthesis with Latent Diffusion Models. *arXiv:2112.10752 [cs.CV]*
- [43] Ying Sheng, Shiyi Cao, Dacheng Li, Coleman Hooper, Nicholas Lee, Shuo Yang, Christopher Chou, Banghua Zhu, Lianmin Zheng, Kurt Keutzer, et al. 2023. S-lora: Serving thousands of concurrent lora adapters. *arXiv preprint arXiv:2311.03285* (2023).
- [44] Mohammad Shoeybi, Mostofa Patwary, Raul Puri, Patrick LeGresley, Jared Casper, and Bryan Catanzaro. 2019. Megatron-lm: Training multi-billion parameter language models using model parallelism. *arXiv preprint arXiv:1909.08053* (2019).
- [45] Vijay Thakkar, Pradeep Ramani, Cris Cecka, Aniket Shivam, Honghao Lu, Ethan Yan, Jack Kosaian, Mark Hoemmen, Haicheng Wu, Andrew Kerr, Matt Nicely, Duane Merrill, Dustyn Blasig, Fengqi Qiao, Piotr Majcher, Paul Springer, Markus Hohnnerbach, Jin Wang, and Manish Gupta. 2023. CUTLASS. <https://github.com/NVIDIA/cutlass>
- [46] torchtune maintainers and contributors. 2024. *torchtune: PyTorch’s finetuning library*. <https://github.com/pytorch/torchtune>
- [47] Alex Wang, Amanpreet Singh, Julian Michael, Felix Hill, Omer Levy, and Samuel R Bowman. 2018. GLUE: A multi-task benchmark and analysis platform for natural language understanding. *arXiv preprint arXiv:1804.07461* (2018).
- [48] Bingyang Wu, Ruidong Zhu, Zili Zhang, Peng Sun, Xuanzhe Liu, and Xin Jin. 2024. {dLoRA}: Dynamically orchestrating requests and adapters for {LoRA} {LLM} serving. In *18th USENIX Symposium on Operating Systems Design and Implementation (OSDI 24)*. 911–927.
- [49] Wencong Xiao, Romil Bhardwaj, Ramachandran Ramjee, Muthian Sivathanu, Nipun Kwatra, Zhenhua Han, Pratyush Patel, Xuan Peng, Hanyu Zhao, Quanlu Zhang, et al. 2018. Gandiva: Introspective cluster scheduling for deep learning. In *13th USENIX Symposium on Operating Systems Design and Implementation (OSDI 18)*. 595–610.
- [50] An Yang, Baosong Yang, Beichen Zhang, Binyuan Hui, Bo Zheng, Bowen Yu, Chengyuan Li, Dayiheng Liu, Fei Huang, Haoran Wei, et al. 2024. Qwen2. 5 technical report. *arXiv preprint arXiv:2412.15115* (2024).
- [51] Justin Zhao, Timothy Wang, Wael Abid, Geoffrey Angus, Arnav Garg, Jeffery Kinnison, Alex Sherstinsky, Piero Molino, Travis Addair, and Devvret Rishi. 2024. LoRA Land: 310 Fine-tuned LLMs that Rival GPT-4, A Technical Report. *arXiv preprint arXiv:2405.00732* (2024).
- [52] Yanli Zhao, Andrew Gu, Rohan Varna, Liang Luo, Chien-Chin Huang, Min Xu, Less Wright, Hamid Shojanazeri, Myle Ott, Sam Shleifer, et al. 2023. Pytorch fsdp: experiences on scaling fully sharded data parallel. *arXiv preprint arXiv:2304.11277* (2023).



## A LoRA memory constraints

### A.1 LoRA Memory Constraints

To ensure that the training job does not exhaust the available GPU memory, we impose a constraint on the total memory used by all LoRA configurations in a job, including the base model weights. The total memory usage must not exceed the GPU memory:

$$M_{\text{base}} + \sum_{k=1}^K M_{\text{lora},k} \leq c_{\text{load}} \times M_{\text{gpu}}$$

$M_{\text{base}}$  represents the memory cost of the base model, while  $M_{\text{lora},k}$  represents the memory cost of a LoRA adapter on a device. Similar to other work on managing GPU memory [31], the user can set a load factor  $c_{\text{load}}$  to account for internal GPU fragmentation and adjust GPU memory usage.

For each LoRA configuration  $k$ , the memory usage,  $M_{\text{lora},k}$ , is represented by an indicator variable to determine if the user applies LoRA to those matrices. In each attention block, the user can apply LoRA to  $Q, K, V$ , and the output projection matrix; In each MLP block, the user can apply LoRA to the up, down, and gate projection matrix. We, therefore, write the LoRA memory usage as a sum of these 7 components:

$$M_{\text{lora},k} = \sum_{i=1}^7 \mathbb{I}_i M_{\text{lora},i} \quad (20)$$

Each index  $i$  corresponds to one of the seven components the user can apply LoRA to. For each component, the LoRA memory usage includes the memory required to store LoRA parameters, gradients, and activations:

$$M_{\text{lora},k} = M_{\text{lora\_param},k} + M_{\text{lora\_grad},k} + M_{\text{lora\_act},k} \quad (21)$$

The memory for LoRA parameters,  $M_{\text{lora\_param},k}$ , is given by:

$$M_{\text{lora\_param},k} = n_{\text{layers}} (h_{\text{in}} \times r_{\text{lora},k} + h_{\text{out}} \times r_{\text{lora},k}) \times c_{\text{prec}}$$

In practice, this may change depending on memory-saving strategies such as activation checkpointing. Here,  $n_{\text{layers}}$  is the number of layers,  $h_{\text{in}}$  and  $h_{\text{out}}$  represent the input and output dimensions of the projection matrix, which can take different values based on the model architecture and vary between attention and MLP blocks.  $c_{\text{prec}}$  is the training precision, representing bytes per parameter.

The memory required for the gradients,  $M_{\text{lora\_grad},k}$ , is calculated as:

$$M_{\text{lora\_grad},k} = c_{\text{grad}} \times M_{\text{lora\_param},k} \times c_{\text{prec}}$$

$c_{\text{grad}}$  represents the scaling factor for storing gradient-related parameters. For example, this factor is three in the popular AdamW optimizer, representing momentum, velocity, and primary gradients.

Finally, the LoRA activation memory for each block,  $M_{\text{lora\_act},i}$ , is given by:

$$M_{\text{lora\_act},k} = b \times s \times r_{\text{lora},k} \times c_{\text{prec}}$$

Here  $b$  is the batch size, and  $s$  is the sequence length. This term represents the memory used to store intermediate activations during training. In LLM fine-tuning, the sequence length varies based on the workload. The standard practice is to set a maximum training length and split the training document if some data samples are too long to ensure no memory overflow. When computing memory consumption, we take the same approach and set the sequence length to the maximum length of the training samples.

Similarly, the activation memory for the base model can be computed by summing the activation of the embedding layer, the attention operator, and the feed-forward network in each layer. Depending on the implementation, other activations, such as those produced by layer norm may also be computed and stored, our model can be adapted to those implementations with ease. More details on computing the memory consumption for each of these four modules can be found in the Appendix:

$$M_{\text{base\_act}} = M_{\text{base\_emb}} + M_{\text{base\_attn}} + M_{\text{base\_mlp}}$$

The total memory for the base model is then calculated as:

$$M_{\text{base}} = M_{\text{base\_weights}} + M_{\text{base\_act}}$$

The computation in this section assumes a single-device setting. The section discusses how the parallelization strategy affects our memory constraints.

#### A.1.1 Parallelization strategy and GPU constraints:

The prior section of constraints assumes that a full copy of the model is stored on each device. In practice, tensor parallelism, pipeline parallelism, and fully-sharded data parallelism (FSDP) are popular strategies to parallelize LLM training and are necessary for modern LLMs. The following section explains how we incorporate different parallelization strategies into our cost model. To accommodate tensor parallelism and pipeline parallelism, we can rewrite the memory cost associated with the LoRA adapters  $i$  as follows:

$$M_{\text{lora\_param},k} = \frac{M_{\text{lora\_param},k}}{d_{\text{tp}} * d_{\text{pp}}}$$

This is similar to base model parameters and intermediate outputs. For FSDP, the model computes the following for different levels of ZeRO optimizers. For ZeRO-1, the LoRA memory includes both the unsharded gradient and parameter memory and the sharded optimizer state:

$$M_{\text{lora},k}^{(1)} = M_{\text{lora\_grad},k}^{(1)} + M_{\text{lora\_param},k} + \frac{M_{\text{opt},k}}{d_{\text{fsdp}}}$$

**Table 8.** In this table, we show the throughput improvement of attention and MLP forward and backward LoRA kernels using sequence length 1024 on A10 GPUs as we scale up the number of concurrent LoRA adapters. The first number in each cell represents the throughput improvement (FLOP/s) of the forward pass, while the second number represents the backward pass.

# LoRA Dim	3B Attention 2048	3B MLP 11008	7B Attention 3584	7B MLP 18944
2	1.98x/1.98x	1.9x/1.86x	1.94x/1.97x	1.98x/1.90x
8	7.65x/7.55x	7.52x/7.42x	7.48x/7.4x	7.44x/7.5x
32	25.95x/26.09x	25.87x/26.14x	27.24x/26.45x	26.78x/26.97x

For ZeRO-2, the gradient memory also includes the gradient term:

$$M_{\text{lora}, k^{(2)}} = M_{\text{lora\_param}, k} + \frac{M_{\text{lora\_grad}, k} + M_{\text{opt}, k}}{d_{\text{fsdp}}}$$

For ZeRO-3, the memory includes all fully sharded components:

$$M_{\text{lora}, k}^{(3)} = \frac{M_{\text{lora\_param}, k} + M_{\text{lora\_grad}, k} + M_{\text{opt}, k}}{d_{\text{fsdp}}}$$

Then, the model will solve for concurrent training jobs to launch and determine each job’s parallelization strategy, ensuring that the total GPU usage does not exceed the GPU constraints.

We apply this formulation to every memory cost computation and add a total GPU constraint where the model will solve for the number of jobs to launch concurrently, as well as the tensor parallel degrees and LoRA adapter configurations to be packed on each job:

$$\sum_j d_j \leq G$$

## B Concurrent LoRA kernels

### B.1 More Kernel Results

In Table 8, we present kernel speed-up as we scale up LoRA forward and backward kernels.

## C Proof of greedy scheduling tail effect

*Proof.* We start by noting that before starting the last job, all  $G$  GPUs are fully utilized by the definition of our greedy scheduling algorithm. Moreover, our algorithm offers a monotonicity condition: if a job using  $x$  GPUs is scheduled, the next job in the optimal ordering requires no more than  $x$  GPUs. This condition guarantees no bubbles between jobs in the fully loaded batches; the only underutilization occurs in the final batch.

Define the total GPU work as  $W = \sum_{j \in J} x_j t_j$ . Recall that  $t_{\text{last}}$  denotes the processing time of the last job and the cumulative time of the fully utilized jobs before starting the last

job be  $F_{\text{prev}}$ . Let  $F = F_{\text{prev}} + t_{\text{last}}$  be the makespan of the job planner’s schedule, and OPT be the makespan of an optimal schedule with full GPU utilization throughout. Then we can write:

$$W = F_{\text{prev}} \cdot G + t_{\text{last}}(G - D),$$

and the total makespan of the greedy schedule is

$$F = F_{\text{prev}} + t_{\text{last}}.$$

An optimal schedule (with full GPU utilization in every batch) must satisfy

$$\text{OPT} \geq \frac{W}{G} = F_{\text{prev}} + t_{\text{last}} \frac{G - D}{G}.$$

Thus, we can bound the extra time incurred due to the bubble in the last batch by

$$F - \text{OPT} \leq [F_{\text{prev}} + t_{\text{last}}] - \left[ F_{\text{prev}} + t_{\text{last}} \frac{G - D}{G} \right] \quad (22)$$

$$= t_{\text{last}} \left( 1 - \frac{G - D}{G} \right) \quad (23)$$

$$= t_{\text{last}} \frac{D}{G} \quad (24)$$

This result quantifies the tail effect under asynchronous scheduling: the extra time is proportional to the fraction of idle GPUs for the last job. And we can obtain our final bound:

$$\frac{F}{\text{OPT}} \leq 1 + \frac{t_{\text{last}} \cdot \frac{D}{G}}{F_{\text{prev}} + t_{\text{last}} \cdot \frac{G - D}{G}} \quad (25)$$

which can be simplified to

$$\frac{F}{\text{OPT}} \leq \frac{F}{F - t_{\text{last}} \cdot \frac{G - D}{G}}.$$

□